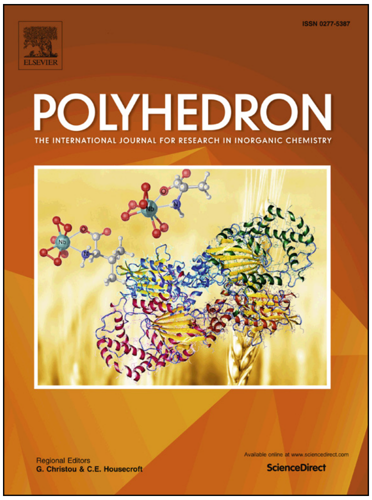

A family of hexanuclear lanthanide complexes with slow magnetic relaxation for Dy_6 cluster

Li-Juan Wu, Hua Yang, Su-Yuan Zeng, Da-Cheng Li, Jian-Min Dou

PII: S0277-5387(17)30192-4
DOI: http://dx.doi.org/10.1016/j.poly.2017.03.012
Reference: POLY 12527

To appear in: *Polyhedron*

Received Date: 6 February 2017
Revised Date: 6 March 2017
Accepted Date: 9 March 2017

Please cite this article as: L-J. Wu, H. Yang, S-Y. Zeng, D-C. Li, J-M. Dou, A family of hexanuclear lanthanide complexes with slow magnetic relaxation for Dy_6 cluster, *Polyhedron* (2017), doi: http://dx.doi.org/10.1016/j.poly.2017.03.012

A family of hexanuclear lanthanide complexes with slow magnetic relaxation for Dy_6 cluster

Li-Juan Wu [a], Hua Yang [a], Su-Yuan Zeng [a], Da-Cheng Li [a,b*], Jian-Min Dou [a,*]

a. School of Chemistry and Chemical Engineering, and Shandong Provincal Key Laboratory of Chemical Energy Storage and Novel Cell Technology, Liaocheng University, Liaocheng, Shangdong 252000, PR China. E-mail: dougroup@163.com; Tel: 0635-8239298.
b. Institute of BioPharmaccutical Research, Liaocheng University, Liaocheng, Shangdong 252059, PR China.

Abstract: A family of isostructural, hexanuclear lanthanide complexes $[Ln_6(L)_4(\mu_3\text{-}OH)_4(CH_3OH)_2(NO_3)_2]$ (Ln = Gd (**1**), Tb (**2**), Dy (**3**), Ho (**4**), Er (**5**), H_3L=1,3-bis(4-methoxysalicylideneamino)-2-propanol) were obtained by the reactions of $Ln(NO_3)_3$ with the selective ligand. Complexes **1−5** were characterized by X-ray single crystal diffraction, IR spectra, and powder X-ray diffraction analyse. The molecule structure of these complexes contains a Ln_6O_6 core ligated by two trinuclear subunits. Direct-current (dc) magnetic susceptibility studies reveal the antiferromagnetic interactions between Lanthanide ions. The in-phase (χ') and out-of-phase (χ'') signals have been observed below 10 K in complex **3**, indicating slow relaxation of the magnetization. The deduced effective energy barrier (U_{eff}/k_B) and relaxation time (τ_0) are 6.17 K and = 4.9×10^{-5} s, respectively.

Keywords: Schiff base ligand; Lanthanide ion; Crystal structure; Single-molecule magnet.

1. Introduction

Since the first single-molecule magnet (SMM) has been discovered in dodecanuclear Mn_{12} cluster [1], considerable efforts of chemists and physicists have been devoted to this field due to the potential applications in high-density data storage [2], molecule-based spintronic devices [3] and quantum computing devices [4]. The large spin ground state (S) and uniaxial (negative) magnetic anisotropy (D), leading to an anisotropy energy barrier (U_{eff}) [5], make for to promote the application of SMMs. However, the contradiction between the large S and negative D values becomes a challenge to obtain such special SMM. To resolve the question, the lanthanide ions, in particular Dy and Tb ions with high spins and intrinsic magnetic anisotropy, attract much interest of researchers. Various lanthanide SMMs from mononuclear to polynuclear complexes have been reported [6], and the largest effective energy barrier of 528 K involved a Dy SMM [7]. To our knowledge, the syntheses of lanthanide SMMs usually are influenced by the ligand field. Thus, it is necessary to explore the magnetic interactions between the bridging group and lanthanide ions.

The syntheses of lanthanide SMMs involve many ligands, such as Schiff base [8], hydrazide [9], hydrazone [10], aldehyde [11], carboxylic acids [12], and so on. The mainly feature of these ligands is that the coordinational donors from the ligands not only bind the lanthanide ions, but also play the bridging role to link the adjacent lanthanide ions. While the Schiff base ligands with the flexibly adjusted primary amine group promote many researchers to focus on the reactions of such ligands with lanthanide metal salts. For instance, Tang Jinkui and the co-authors reported a series of Dy SMMs [13]. Among them, a Dy_6 cluster was synthesized based on 1,3-bis(salicylideneamino)-2-propanol and shows SMM behavior [14].

Our group is also interested in Schiff base ligands, and reported two nickel Schiff base complexes with a missing vertices dicubane-like Ni_4O_4 core and a hexanuclear cluster with two nickel ions attaching to a Ni_4O_4 cubane [15]. To continue our study, herein, we synthesized a new multisite Schiff base ligand 1,3-bis(4-methoxysalicylideneamino)-2-propanol (H_3L), and represent a new family of hexanuclear lanthanide clusters $[Ln_6(L)_4(\mu_3\text{-}OH)_4(CH_3OH)_2(NO_3)_2]$ (Ln = Gd (**1**), Tb (**2**), Dy (**3**), Ho (**4**), Er (**5**)). They are isostructural with two triangle Ln_3 units linked by oxygen atoms from μ_3-OH^- units and the alkoxy groups of ligands. Moreover, the magnetic properties are discussed in detail.

2. Experimental section

2.1. Materials and physical methods

The reagents used in the experiments are all analytical grade as purchased from commercial sources. Melting points test was performed by Kofler micro-melting point apparatus. Elemental analyses of C, H and N were determined using an Elemental Vario EL analyzer. The IR spectra were recorded on a PerkinElmer Spectrum with KBr in the 400–4000 cm^{-1}. The magnetic susceptibility was measured on polycrystalline samples with the Quantum Design SQUID magnetometer MPMSXL in the temperature range 1.8–300 K under an applied field of 1kOe. Alternating current (ac) susceptibility measurements for complexes **1–5** were carried out in the frequency range 1–999 Hz under zero dc field.

2.2. X-ray crystallography

Crystallographic diffraction data for **1–5** were performed on a Bruker Smart CCD area-detector diffractometer with Mo-Kα radiation (λ = 0.71073 Å) at room temperature. The program SAINT was used for integration of the diffraction profiles, and the semiempirical absorption corrections were applied using SADABS [16]. All the structures were solved by direct methods using SHELXS-97 and refined against F^2 by full-matrix least-squares methods with SHELXS-97 [17]. Crystallographic data for complexes **1**–**5** have been deposited to the Cambridge Crystallographic Data Centre (CCDC) as supplementary publication numbers: CCDC-1522934 (**1**), 1522828 (**2**), 1522827 (**3**), 1522830 (**4**) and 1522944 (**5**).

2.3. Syntheses

2.3.1. Synthesis of 1,3-bis(4-methoxysalicylideneamino)-2-propanol (H_3L)

A solution of 4-methoxy salicylaldehyde (1.0 mmol) and 1,3-diaminopropan-2-ol (0.5 mmol) was stirred at room temperature in 10 mL of methanol for 2 hour. The resulting yellow solid was filtered and dried in a vacuum. Yield: 109 mg , 60.9%. M.p. 151□. *Anal*. Calc. (%) for $C_{19}H_{22}N_2O_5$: C, 43.58; H, 6.15; N, 7.82. Found (%): C, 43.34; H, 6.08; N, 7.68. IR (KBr): ν (cm^{-1}) = 3431 (br), 3137 (br), 1644 (s), 1522 (s), 1485 (w), 1441 (w), 1367 (w), 1325 (m), 1291 (w), 1222 (s), 1168 (m), 1114 (m), 1020 (m), 967 (w), 875 (w), 838 (m), 785 (w), 578 (w), 465 (w).

2.3.2. Synthesis of $[Gd_6(L)_4(\mu_3\text{-}OH)_4(CH_3OH)_2(NO_3)_2]$ (**1**)

$Gd(NO_3)_3\cdot 6H_2O$ (91.2 mg, 0.2 mmol) and Schiff base ligand (H_3L) (0.0358 g, 0.1 mmol) was reacted in the mixed solution of 1:1 methanol/acetonitrile in the present of sodium hydroxide. The solution was stirred for 5 hours at room temperature and filtered. The filtrate was left undisturbed to allow slow evaporation of the solvent. Yellow single crystals suitable for X-ray diffraction were obtained after a week. Yield: 36 mg, 41.2% (based on Gd). *Anal*. Calc. (%) for $C_{78}H_{88}Gd_6N_{10}O_{32}$: C, 35.71; H, 3.36; N, 5.34. Found (%): C, 35.66; H, 3.28; N, 5.30. IR (KBr): ν (cm^{-1}) = 3422 (br), 2892 (w), 2838 (w), 1624 (s), 1544 (m), 1488 (w), 1443 (w), 1384 (w), 1344 (w), 1301 (w), 1215 (s), 1169 (m), 1122 (m), 1034 (s), 976 (s), 913 (w), 837 (m), 791 (w), 743 (w), 705 (w), 474 (w).

2.3.3. Synthesis of $[Tb_6(L)_4(\mu_3\text{-}OH)_4(CH_3OH)_2(NO_3)_2]$ (**2**)

The complex **2** was obtained by following the procedure for **1** except that $Tb(NO_3)_3\cdot 6H_2O$ (90.6 mg, 0.2 mmol) was used instead of $Gd(NO_3)_3\cdot 6H_2O$, and yellow single crystals suitable for X-ray diffraction were obtained after a week. Yield: 36 mg, 41% (based on Tb). *Anal*. Calc. (%) for $C_{78}H_{88}Tb_6N_{10}O_{32}$: C, 35.57; H, 3.34; N, 5.32. Found (%): C, 35.45; H, 3.25; N, 5.26. IR (KBr): ν (cm^{-1}) = 3425 (br), 2893 (w), 2838 (w), 1625 (s), 1544 (m), 1488 (w), 1443 (w), 1384 (m), 1343 (w), 1301 (m), 1216 (s), 1169 (m), 1122 (s), 1030 (s), 977 (s), 911 (w), 838 (m), 792 (w), 744 (w), 705 (w), 639 (w), 618 (vw), 601 (vw), 582 (w), 474 (w).

2.3.4. Synthesis of $[Dy_6(L)_4(\mu_3\text{-}OH)_4(CH_3OH)_2(NO_3)_2]$ (**3**)

The complex **3** was obtained by following the procedure for **1** except that $Dy(NO_3)_3\cdot 6H_2O$ (91.3 mg, 0.2 mmol) was used instead of $Gd(NO_3)_3\cdot 6H_2O$, and yellow single crystals suitable for X-ray diffraction were obtained after a week. Yield: 31 mg, 35% (based on Dy). *Anal*. Calc. (%) for $C_{78}H_{88}Dy_6N_{10}O_{32}$: C, 35.29; H, 3.32; N, 5.28. Found (%): C, 35.13; H, 3.16; N, 5.17. IR (KBr): ν (cm^{-1}) = 3431 (br), 2894 (w), 2839 (w), 1625 (s), 1605 (s), 1544 (m), 1488 (w), 1443 (w), 1384 (m), 1302 (w), 1216 (s), 1169 (w), 1122 (m), 1031 (m), 977 (m), 913 (w), 838 (m), 792 (w), 744 (w), 706 (w), 640 (vw), 619 (vw), 582 (vw), 475 (w).

2.3.5. Synthesis of $[Ho_6(L)_4(\mu_3\text{-}OH)_4(CH_3OH)_2(NO_3)_2]$ (**4**)

The complex **4** was obtained by following the procedure for **1** except that $Ho(NO_3)_3\cdot 6H_2O$ (91.8 mg, 0.2 mmol) was used instead of $Gd(NO_3)_3\cdot 6H_2O$, and yellow single crystals suitable for X-ray diffraction were obtained after a week. Yield: 26 mg, 29.3% (based on Ho). *Anal*. Calc. (%) for $C_{78}H_{88}Ho_6N_{10}O_{32}$: C, 35.09; H, 3.30; N, 5.25. Found (%): C, 34.91; H, 3.14; N, 5.09. IR (KBr): ν (cm^{-1}) = 3440 (br), 2895 (w), 2839 (w), 1625 (s), 1545 (m), 1488 (w), 1443 (w), 1384 (m), 1296 (m), 1217 (s), 1169 (w), 1123 (m), 1031 (s), 977 (s), 912 (w), 839 (m), 792 (w), 744 (w), 706 (w), 641 (w), 619 (w), 583 (w), 475 (w).

2.3.6. Synthesis of $[Er_6(L)_4(\mu_3\text{-}OH)_4(CH_3OH)_2(NO_3)_2]$ (**5**)

The complex **5** was obtained by following the procedure for **1** except that $Er(NO_3)_3\cdot 6H_2O$ (92.3 mg, 0.2 mmol) was used instead of $Gd(NO_3)_3\cdot 6H_2O$, and yellow single crystals suitable for X-ray diffraction were obtained after a week. Yield: 21 mg, 23.5% (based on Er). *Anal*. Calc. (%) for $C_{78}H_{88}Er_6N_{10}O_{32}$: C, 34.91; H, 3.28; N, 5.22. Found (%): C, 34.76; H, 3.09; N, 5.04. IR (KBr): ν (cm^{-1}) = 3423 (br), 3001 (vw), 2896 (w), 2839 (w), 1625 (s), 1546 (s), 1488 (w), 1444 (w), 1425 (w), 1384 (m), 1296 (m), 1217 (s), 1169 (m), 1123 (s), 1061 (w), 1030 (s), 977 (s), 912 (w), 839 (m), 792 (w), 744 (w), 705 (w), 641 (w), 620 (vw), 602 (vw), 584 (w), 476 (w).

Table 1. Crystallographic data and structure refinement parameters for **1**–**5**

	1	**2**	**3**	**4**	**5**
chemical formula	$C_{78}H_{88}Gd_6N_{10}O_{32}$	$C_{78}H_{88}Tb_6N_{10}O_{32}$	$C_{78}H_{88}Dy_6N_{10}O_{32}$	$C_{78}H_{88}Ho_6N_{10}O_{32}$	$C_{78}H_{88}Er_6N_{10}O_{32}$
fw g mol^{-1}	2621.08	2631.10	2652.58	2667.16	2681.14
temp/K	298(2)	298(2)	298(2)	298(2)	298(2)

cryst syst	Orthorhombic	Orthorhombic	Orthorhombic	Orthorhombic	Orthorhombic
space group	Pbca	Pbca	Pbca	Pbca	Pbca
a/ Å	21.4451(19)	21.5670(16)	21.3279(19)	21.3479(19)	21.3096(19)
b /Å	21.4682(19)	21.4663(15)	21.7651(19)	21.7411(19)	21.5382(19)
c/ Å	21.7371(18)	21.7785(17)	21.4700(18)	21.4093(17)	21.8558(18)
β/deg	90	90	90	90	90
volume/ $Å^3$	10007.5(15)	10082.7(13)	9966.5(15)	9936.6(15)	10031.2(15)
Z	4	4	4	4	4
D_c(Mg m^{-3})	1.740	1.733	1.768	1.783	1.775
μ /mm^{-1}	3.997	4.229	4.519	4.798	5.040
Data/parameters	8723/573	8887/573	8788/574	8747/573	8401/525
$F(000)$	5064	5088	5112	5136	5160
R_{int}	0.1177	0.0933	0.0000	0.1151	0.2211
R_1 [I>2σ(I)]	0.0841	0.0624	0.1303	0.0816	0.2077
wR_2 (all data)	0.2466	0.1782	0.3199	0.2451	0.5310
GOF on F^2	0.926	1.074	0.952	0.985	1.317

3. Results and discussion

3.1. Syntheses and crystal structures analysis

The Schiff base ligand 1,3-bis(4-methoxysalicylideneamino)-2-propanol (H_3L) exhibits the pentadentate N_2O_3 donor set and possesses the chelating and bridging capacities. Complexes **1–5** were synthesized by the reactions of the Schiff base ligand (H_3L) and lanthanide nitrate salts in a 1:2 ratio with the present of NaOH in methanol/acetonitrile mixture solution at room temperature. The purity of the single-crystal samples was determined by the powder X-ray diffraction analyses (Fig. S6). By comparing and analyzing the diffraction peaks between experimental and simulated patterns prove that the samples are pure.

3.2. Molecular structures of complexes **1–5**

The molecular structures of complexes **1–5** were determined by X-ray single-crystal analysis. Five complexes are isomorphs and crystallize in orthorhombic space group Pbca with Z = 4. The crystallographic data and structure refinement details for complexes **1–5** are summarized in Table 1. The selected bond distances and angles are shown in Table S1–S5. Herein, the molecular structure of complex **3** is described in detail as a representative example.

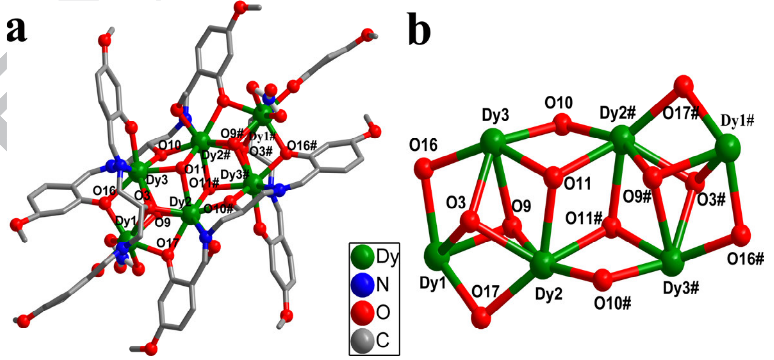

Fig. 1. (a) Partially labeled crystal structure of complex **3** with hydrogen atoms omitted for clarity. (b) Dy_6 core in complex **3**.

Complex **3** consists of six Dy ions, four deprotonated Schiff base ligands, two nitrate anions, two coordinated methanol molecules, and four bridged μ_3-OH^- (Fig. 1a). The structure is centrosymmetric and contains a hexanuclear $[Dy_6(\mu_3\text{-}OH)_4(\mu_3\text{-}O_{alkoxy})_2]^{12+}$ core with two trinuclear subunits $[Dy_3(\mu_3\text{-}OH)(\mu_3\text{-}O_{alkoxy})]^{7+}$ building blocks fused together through μ_3-OH^- oxygen atoms (O11 and O11#) and alkoxy oxygen atoms (O10 and O10#). The similar structure has been reported in literatures[18]. The μ_3-OH^- units are involved in encapsulated inside bridging three neighboring Dy ions (Dy1, Dy2 and Dy3; Dy2, Dy3 and Dy2#) (Fig. 1b). Four Schiff base ligands adopt two coordinate and bridging modes, such as μ_3-η_1:η_1:η_3:η_1:η_1 linking three Dy ions (Dy1, Dy2 and Dy3) and μ_4-η_2:η_1:η_2:η_1:η_2 holding four Dy ions (Dy1, Dy2, Dy3# and Dy1#). The phenolate and alkoxy oxygen atoms (O10, O16 and O17) of the ligands play the bridging role to link the adjacent Dy ions (Dy3 and Dy2#, Dy1 and Dy3, Dy1 and Dy2) at the edge. Three different types of oxygen atoms are coordinated to each Dy ion. The average bond distances are Dy–μ_3-O$_{\text{hydroxo}}$ = 2.38 Å, Dy–O$_{\text{phenolate}}$ = 2.30 Å and Dy–O$_{\text{alkoxy}}$ = 2.35 Å, which are similar to those found in literatures [19]. The Dy–N bond lengths are in the range of 2.46-2.58 Å. Each Dy ion is eight-coordinate with the coordination positions of Dy1 occupied by NO7 donor atoms from one μ_3-η_1:η_1:η_3:η_1:η_1 ligand, two μ_4-η_2:η_1:η_2:η_1:η_2 ligands, one nitrate anions and one μ_3-OH$^-$. Dy2 is surrounded by one oxygen atom from μ_3-η_1:η_1:η_3:η_1:η_1 ligand, one nitrogen atom and two oxygen atoms from μ_4-η_2:η_1:η_2:η_1:η_2 ligand, three oxygen atoms from three μ_3-OH$^-$, and one oxygen atom from coordinated methanol molecular. Dy3 is coordinated by two phenolate oxygen, two alkoxy oxygen atoms, two μ_3-OH$^-$ oxygen atoms, and two imino nitrogen atoms from the μ_3-η_1:η_1:η_3:η_1:η_1 ligand and μ_4-η_2:η_1:η_2:η_1:η_2 ligand. The intramolecular Dy···Dy distances are in the range of 3.52–3.99 Å. The Dy–O–Dy bond angles are in the range 93.8(6)–114.5(6)°. Furthermore, The adjacent molecules are connected by O8···H28A–C28 to give a 1–D supramolecular chain. These supramolecular chains are further interconnected through weak O4···H32–C32 interactions to afford a 2–D supramolecular architecture. Complexes **1**–**5** are the same type of 2–D supramolecular architectures (Fig. S1-S5).

3.3. Magnetic properties

The temperature-dependent dc magnetic susceptibility data for complexes **1**–**5** was performed in the temperature range 1.8–300 K under an applied magnetic field of 1 kOe. The collected data is plotted as $\chi_M T$ *versus* T in Fig. 2a. For **1**, the observed $\chi_M T$ value is 43.55 cm^3 K mol^{-1} at 300 K, lower than the expected value of 47.25 cm^3 K mol^{-1} for six free Gd^{III} ($^8S_{7/2}$, g = 2). With the temperature decreasing, the $\chi_M T$ value remains fairly constant until down to 50 K, and then drops rapidly to 17.62 cm^3 K mol^{-1} at 2 K. The behavior can be attributed to the presence of the intramolecular antiferromagnetic interactions between the Gd ions because the isotropic nature of Gd ions. The curve of χ_M^{-1}–T is almost a linear and can be fitted by Curie-Weiss law $\chi = C/(T - \theta)$ where the constants are C = 44.40 cm^3 K mol^{-1} and θ = -2.17 K, respectively. The negative Weiss constant further confirmed the antiferromagnetic interactions between the Gd ions. For complexes **2–5**, the observed $\chi_M T$ values are 62.93(**2**), 78.97(**3**), 79.09(**4**) and 65.41(**5**) cm^3 K mol^{-1} at 300K, respectively, which are lower than the expected values for six noninteracting Ln^{III} [Tb^{III}, ($^7F_6$, g = 3/2); Dy^{III}, ($^6H_{15/2}$, g = 4/3); Ho^{III}, ($^5I_8$, g = 5/4) and Er^{III}, ($^4I_{15/2}$, g = 6/5)] ions of 70.92, 85.02, 84.42 and 69.0 cm^3 K mol^{-1}. As the temperature lowers, the $\chi_M T$ values remain almost invariable over a broad temperature, then gradually decrease to 33.69 (**2**), 58.12 (**3**), 54.52 (**4**) and 27.59 (**5**) cm^3 K mol^{-1} at 2 K, respectively. This behavior is mainly associated with the thermal depopulation of the Stark sublevels, which are originated from the crystal field. Therefore, the nature of the interactions between the lanthanide ions could not be determined from the shape of the $\chi_M T$ *versus* T curve.

The field dependence of magnetizations of complexes were investigated in the range 0–50 kOe at 3K. The plots of M *versus* H for **2–5** are shown in Fig. 2b. The magnetizations of complexes **2–5** demonstrate a rapid increase in the initial stage, and then increase linearly to reach 25.77 (**2**), 29.73 (**3**), 28.61 (**4**) and 26.53 (**5**) μ_B at 50 kOe without clear saturation, respectively. The non-superposition of the M *versus* H/T plots (Fig. S7-S10) on a single master curve suggests the presence of significant magnetic anisotropy and/or low-lying excited states in the systems.

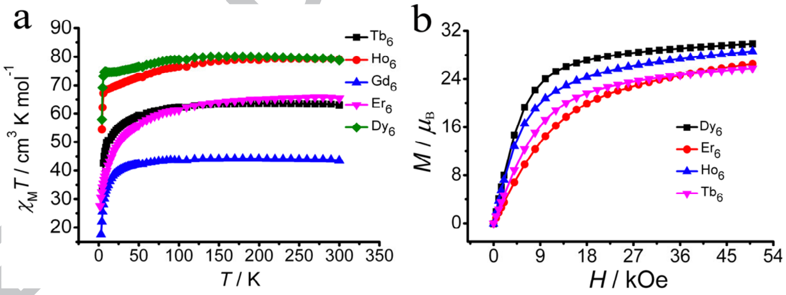

Fig. 2. (a) Temperature dependence of $\chi_M T$ *vs.* T curves for **1–5** under an applied magnetic field of 1000 Oe. (b) Field dependence of the magnetization for **2–5** obtained at 3 K.

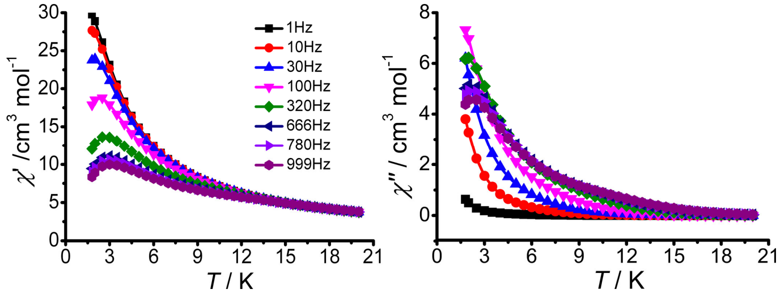

Fig. 3. Temperature dependence of the in-phase (χ') and out-of-phase (χ'') signals under zero dc field for **3**.

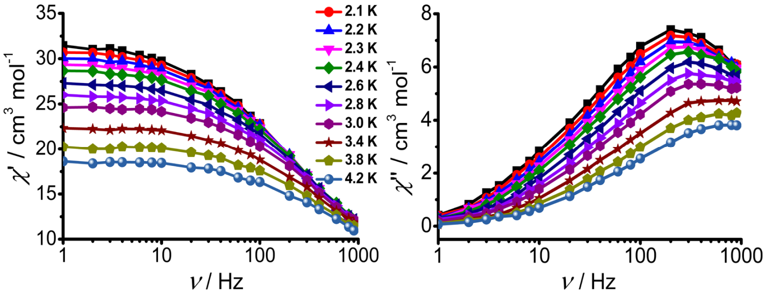

Fig. 4. Frequency dependence of the in-phase (χ') and out-of-phase (χ'') signals under zero dc field for **3.**

In order to probe the magnetic dynamic behavior, the ac magnetization susceptibility studies of complexes **1–5** were carried out under a zero applied dc field. Temperature dependence of the in-phase (χ') and out-of-phase (χ'') signals between 1 and 999 Hz are observed for complex **3** under zero dc field below 15K, suggesting slow relaxation of the magnetization, a typical of SMM behavior (Fig. 3). The frequency-dependent ac susceptibility of **3** is also depicted in Fig. 4. The magnetization relaxation time (τ) can be extracted from frequency-dependent ac susceptibility, where $\tau = 1/(2\pi\nu)$ (ν is the corresponding frequency of maximum χ'' at different temperatures). According to the Arrhenius law [$\tau = \tau_0 \exp(U_{\mathrm{eff}}/k_{\mathrm{B}}T)$], the fitting of ln$\tau$ *versus* $1/T$ plot was given in Fig. 5. It can be calculated that the energy barrier ($U_{\mathrm{eff}}/k_{\mathrm{B}}$) is 6.17 K and the pre-exponential factor (τ_0) is 4.9×10^{-5} s.

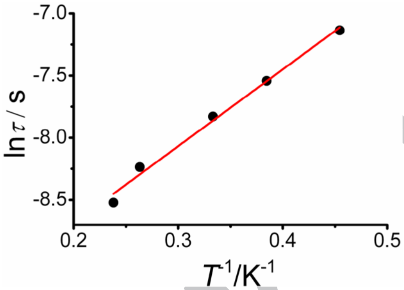

Fig. 5. Plot of lnτ *vs.* T^{-1} fitting to the Arrhenius law for complex **3**.

4. Conclusion

In summary, five hexanuclear lanthanide complexes [$\mathrm{Ln_6(L)_4(\mu_3\text{-}OH)_4(CH_3OH)_2(NO_3)_2}$] have been synthesized and characterized. The structures analyses revealed that five complexes are isostructural and six Ln ions are linked together by μ_3-OH$^-$ oxygen atoms and phenolate or alkoxy with four μ_3-OH$^-$ units encapsulated inside to form a $\mathrm{Ln_6O_6}$ core. The investigation of magnetic studies revealed antiferromagnetic interactions between Ln ions, and ac susceptibility measurements showed that only complex **3** shows SMM behavior. The calculated effective energy barrier ($U_{\mathrm{eff}}/k_{\mathrm{B}}$) and relaxation time pre-exponential factor are 6.17 K and $\tau_0 = 4.9 \times 10^{-5}$ s, respectively.

Appendix A. Supplementary data

CCDC 1522934, 1522828, 1522827, 1522830 and 1522944 contain the supplementary crystallographic data for **1–5**. These data can be obtained free of charge via http://www.ccdc.cam.ac.uk/conts/retrieving.html, or from the Cambridge Crystallographic Data Centre, 12 Union Road, Cambridge CB2 1EZ, UK; fax: (+44) 1223-336-033; or e-mail: deposit@ccdc.cam.ac.uk.

Acknowledgements

This work was supported by the National Natural Science Foundation of China [grant No. 21671093 and 21271097]; Shandong “Tai-Shan Scholar Research Fund” and Liaocheng University.

References

[1] (a) R. Sessoli, D. Gatteschi, A. Caneschi, M.A. Novak, Nature. 365 (1993) 141;
(b) R. Sessoli, H.L. Tsai, A.R. Schake, S. Wang, J.B. Vincent, K. Folting, D. Gatteschi, G. Christou, D.N. Hendrickson, J. Am. Chem. Soc. 115 (1993) 1804.
[2] (a) M. Jenkins, T. Huemmer, M.J. Martinez-Perez, J. Garcia-Ripoll, D. Zueco, F. Luis, New J. Phys. 15 (2013) 095007;
(b) J.D. Rinehart, M. Fang, W.J. Evans, J.R. Long, J. Am. Chem. Soc. 36 (2011) 14236.

[3] (a) L. Bogani, R. Maurand, L. Marty, C. Sangregorio, C. Altavilla, W. Wernsdorfer, J. Mater. Chem. 20 (2010) 2099;
(b) S. DeFranceschi, L. Kouwenhoven, C. Schoenenberger, W. Wernsdorfer, Nat. Nanotechnol. 5 (2010) 703;
(c) K. Hong, W.Y. Kim, Angew. Chem. Int. Ed. 52 (2013) 3389.
[4] (a) G. Aromí, D. Aguilà, P. Gamez, F. Luisc, O. Roubeauc, Chem. Soc. Rev. 41 (2012) 537;
(b) M.N. Leuenberger, D. Loss, Nat. 410 (2001) 789;
(c) J. Lehmann, A. Gaita-Ariño, E. Coronado, D. Loss, J. Mater. Chem. 19 (2009) 1672;
(d) L. Bogani, W. Wernsdorfer, Nat. Mater. 7 (2008) 179.
[5] (a) B. Joarder, S. Mukherjee, S.F. Xue, J.K. Tang, S.K. Ghosh, Inorg. Chem. 53 (2014) 7554;
(b) P. Zhang, Y.N. Guo, J.K. Tang, Coord. Chem. Rev. 257 (2013) 1728.
[6] (a) J. Luzona, R. Sessoli, Dalton Trans. 41 (2012) 13556;
(b) D.N. Woodruff, R.E.P. Winpenny, R.A. Layfield, Chem. Rev. 113 (2013) 5110.
[7] R.J. Blagg, C.A. Muryn, E.J.L. McInnes, F. Tuna, R.E.P. Winpenny, Angew. Chem. Int. Ed. 50 (2011) 6530.
[8] (a) S. Das, A. Dey, S. Biswas, E. Colacio, V. Chandrasekhar, Inorg. Chem. 53 (2014) 3417;
(b) L. Zhao, S.F. Xue, J.K. Tang, Inorg. Chem. 51 (2012) 5994;
(c) S. Mukherjee, A.K. Chaudhari, S.F. Xue, J.K. Tang, S.K. Ghosh, Inorg. Chem. Commun. 35 (2013) 144.
[9] (a) S. Das, S. Hossain, A. Dey, S. Biswas, J.P. Sutter, V. Chandrasekhar, Inorg. Chem. 53 (2014) 5020;
(b) V. Chandrasekhar, S. Das, A. Dey, S. Hossain, J.P. Sutter, Inorg. Chem. 52 (2013) 11956;
(c) V. Chandrasekhar, S. Hossain, S. Das, S. Biswas, J.P. Sutter, Inorg. Chem. 52 (2013) 6346;
(d) H.X. Zhang, S.Y. Lin, S.F. Xue, C. Wang, J.K. Tang, Dalton Trans. 43 (2014) 6262.
[10] (a) Y.N. Guo, X.H. Chen, S.F. Xue, J.K. Tang, Inorg. Chem. 50 (2011) 9705;
(b) S.F. Xue, X.H. Chen, L. Zhao,Y.N. Guo, J.K. Tang, Inorg. Chem. 51 (2012) 13264;
(c) S.F. Xue, L. Zhao, Y.N. Guo, X.H. Chen, J.K. Tang, Chem. Commun. 48 (2012) 7031;
(d) S.Y. Lin, L. Zhao, Y.N. Guo, P. Zhang, Y. Guo, J.K. Tang, Inorg. Chem. 51 (2012) 10522.
[11] (a) I.J. Hewitt, J.K. Tang, N.T. Madhu, C.E. Anson, Y.H. Lan, J. Luzon, M. Etienne, R. Sessoli, A.K. Powell, Angew. Chem. Int. Ed. 49 (2010) 6352;
(b) J.K. Tang, I. Hewitt, N.T. Madhu, G. Chastanet, W. Wernsdorfer, C.E. Anson, C. Benelli, R. Sessoli, A.K. Powell, Angew. Chem. Int. Ed. 45 (2006) 1729 .
[12] (a) Y.J. Gao, G.F. Xu, L. Zhao, J.K. Tang, Z.L. Liu, Inorg. Chem. 48 (2009) 11495;
(b) X.M. Zhang, K. Wang, Y.Q. Wang, E.Q. Gao, Dalton Trans., 40 (2011) 12742;
(c) Q.W. Li, J.L. Liu, J.H. Jia, J.D. Leng, W.Q. Lin, Y.C. Chen, M.L. Tong, Dalton Trans. 42 (2013) 11262;
(d) M. Fang, J.J. Li, P.F. Shi, B. Zhao, P. Cheng, Dalton Trans. 42 (2013) 6553.
[13] (a) L. Zhao, J.F. Wu, H.S. Ke, J.K. Tang, CrystEngComm. 15 (2013) 5301;
(b) L. Zhang, P. Zhang, L. Zhao, S.Y. Lin, S.F. Xue, J.K. Tang, Z.L. Liu, Eur. J. Inorg. Chem. 8 (2013) 1351;
(c) S.Y. Lin, C. Wang, L. Zhao, J.F. Wu, J.K. Tang, Dalton Trans. 44 (2015) 223.
[14] H.S. Ke, L. Zhao, Y. Guo, J.K. Tang, Eur. J. Inorg. Chem. 27 (2011) 4153.
[15] S.Z. Liu, S.N. Wang, F. Cao, H.Y. F, D.C. Li, J.M. Dou, RSC Advances. 2 (2012) 1310.
[16] (a) SAINT v5.0-6.01, Bruker Analytical X-ray Systems Inc., Madison, WI, 1998;
(b) G. M. Sheldrick, SADABS, University of Göttingen, Göttingen, Germany.
[17] (a) J, Schraml, Appl. Organomet. Chem. 14 (2000) 604;
(b) SHELXTL v5.1, Bruker Analytical X-ray Systems Inc., Madison, WI, 1999.
[18] (a) X.L. Li, H. Li, D.M. Chen, C. Wang, J.F. Wu, J.K. Tang, W. Shi, P. Cheng, Dalton Trans. 44 (2015) 20316;
(b) X.L. Li, J.F. Wu, J.K. Tang, B.L. Guennic, W. Shi, P. Cheng, Chem. Commun. 52 (2016) 9570.
[19] (a) V. Chandrasekhar, S. Hossain, S. Das, S. Biswas, J.-P. Sutter, Inorg. Chem. 52 (2013) 6346;
(b) V. Chandrasekhar, S. Das, A. Dey, S. Hossain, J.-P. Sutter, Inorg. Chem. 52 (2013) 11956;
(c) H.Q. Tian, Y.N. Guo, L. Zhao, J.K. Tang, Z.L. Liu, Inorg. Chem. 50 (2011) 8688.
(d) S. Das, S. Hossain, A. Dey, S. Biswas, J.-P. Sutter, V. Chandrasekhar, Inorg. Chem. 53 (2014) 5020.

Graphical abstract

A family of hexanuclear lanthanide complexes with slow magnetic relaxation for Dy_6 cluster

Li-Juan Wu [a], Hua Yang [a], Su-Yuan Zeng [a], Da-Cheng Li [a,b*], Jian-Min Dou [a,*]

a. School of Chemistry and Chemical Engineering, and Shandong Provincal Key Laboratory of Chemical Energy Storage and Novel Cell Technology, Liaocheng University, Liaocheng, Shangdong 252000, PR China. E-mail: dougroup@163.com; Tel: 0635-8239298.
b. Institute of BioPharmaccutical Research, Liaocheng University, Liaocheng, Shangdong 252059, PR China.

Five isostructural hexanuclear lanthanide complexes $[Ln_6(L)_4(\mu_3\text{-}OH)_4(CH_3OH)_2(NO_3)_2]$ (Ln=Gd (**1**), Tb (**2**), Dy (**3**), Ho (**4**), Er (**5**)) based on 1,3-bis(4-methoxysalicylideneamino)-2-propanol (H_3L) have been synthesized and characterized. Each structure contains a Ln_6O_6 core with two trinuclear subunits fused together through μ_3-O atoms. The magnetic properties reveal slow relaxation of magnetization in complex **3**.